Ultrafast Carotenoid-to-Chlorophyll Singlet Energy Transfer in the Cytochrome b_6f Complex from *Bryopsis corticulans*

Ping Zuo,* Bin-Xing Li,[†] Xiao-Hui Zhao,* Yi-Shi Wu,* Xi-Cheng Ai,* Jian-Ping Zhang,* Liang-Bi Li,[†] and Ting-Yun Kuang[†]

*State Key Laboratory for Structural Chemistry of Unstable and Stable Species, Institute of Chemistry, Chinese Academy of Sciences, Beijing 100080, People's Republic of China; and [†]Key Laboratory of Photosynthesis and Environmental Molecular Physiology, Institute of Botany, Chinese Academy of Sciences, Beijing 100093, People's Republic of China

ABSTRACT   Ultrafast carotenoid-to-chlorophyll (Car-to-Chl) singlet excitation energy transfer in the cytochrome b_6f (Cyt b_6f) complex from *Bryopsis corticulans* is investigated by the use of femtosecond time-resolved absorption spectroscopy. For all-*trans*-α-carotene free in *n*-hexane, the lifetimes of the two low-lying singlet excited states, $S_1(2A_g^-)$ and $S_2(1B_u^+)$, are determined to be 14.3 ± 0.4 ps and 230 ± 10 fs, respectively. For the Cyt b_6f complex, to which 9-*cis*-α-carotene is bound, the lifetime of the $S_1(2A_g^-)$ state remains unchanged, whereas that of the $S_2(1B_u^+)$ state is significantly reduced. In addition, a decay-to-rise correlation between the excited-state dynamics of α-carotene and Chl *a* is clearly observed. This spectroscopic evidence proves that the $S_2(1B_u^+)$ state is able to transfer electronic excitations to the Q_x state of Chl *a*, whereas the $S_1(2A_g^-)$ state remains inactive. The time constant and the partial efficiency of the energy transfer are determined to be 240 ± 40 fs and (49 ± 4)%, respectively, which supports the overall efficiency of 24% determined with steady-state fluorescence spectroscopy. A scheme of the α-carotene-to-Chl *a* singlet energy transfer is proposed based on the excited-state dynamics of the pigments.

INTRODUCTION

The cytochrome b_6f (Cyt b_6f) complex is an oxidoreductase in the thylakoid membrane. It catalyzes the electron transfer from plastoquinol to plastocyanin and generates a transmembrane proton gradient utilized for the ATP synthesis (1,2). In addition, this complex is responsible for a balance of the amount of light excitation between photosystem II (PS II) and photosystem I (PS I) by regulating the kinase activation of the PS II light-harvesting complex (LHC II) (3). Crystallographic structures of Cyt b_6f complexes from the thermophilic cyanobacterium *Mastigocladus laminosus* (4) and the green alga *Chlamydomonas reinhardtii* (5) show that a monomeric Cyt b_6f consists of four large subunits (Cyt *f*, Cyt b_6, Rieske iron-sulfur protein, and subunit IV), four small hydrophobic subunits (Pet G, Pet L, Pet M, and Pet N), one chlorophyll *a* (Chl *a*) molecule, and one carotenoid (Car) molecule.

Different kinds of Cars have been found in the Cyt b_6f complexes from various species. It has been shown that the Car in spinach Cyt b_6f is a 9-*cis*-β-carotene (6). The presence of β-carotene in the Cyt b_6f complexes from *M. laminosus* and *C. reinhardtii*, as reported by Zhang et al. (7), is corroborated by the recent crystallographic structures (4,5). In addition, eichinenone was found for the cyanobacterium *Synechocystis* sp. PCC 6803 (8) and 9-*cis*-α-carotene for the intertidal green alga *Bryopsis corticulans* (9).

Cars ubiquitously present in natural photosynthetic organisms where they perform dual roles of light harvesting and photoprotection (10,11). In the Cyt b_6f complexes, β-carotene was found to be able to protect the photobleach of Chl *a* in the presence of oxygen, suggesting its role of photoprotection (7). In relation to photoprotection, the chlorophyll-to-carotenoid (Chl-to-Car) triplet excitation energy transfer (EET) was observed for the Cyt b_6f complex from spinach (12) but not for that from *Synechocystis* sp. PCC 6803 (13). As for light harvesting, it was shown that β-carotene cannot transfer singlet excitation energy to Chl *a* in the Cyt b_6f complex from *C. reinhardtii* (14); however, it does so in that from *M. laminosus* although with an extremely low efficiency (7). Since a light-assisted reaction involving Car or Chl *a* seems unnecessary for Cyt b_6f complex to perform physiological functions, the role of the photosynthetic pigments has been mysterious and has attracted considerable research interest (15,16).

The light-harvesting function of Car in photosynthetic pigment-protein complexes has been extensively studied (for reviews, see Frank and Cogdell (10), Ritz et al. (11), and Polívka and Sundström (17)). In bacterial light-harvesting complexes where Cars are mainly in all-*trans* configuration, the overall efficiency of Car-to-BChl EET varies from ~30% to near unity depending on the bacterium (10). Recently, it was shown that 15-*cis* spheroidene transfers singlet excitation to BChl with an overall efficiency of ~75% in the reaction center from wild-type *Rhodobater sphaeroides* (18). In the light-harvesting complexes from higher plants and algae, the overall carotenoid-to-chlorophyll (Car-to-Chl) EET efficiency is ~30% for the CP43 and the CP47 complexes from spinach (19,20), ~80% for the LHC II complex

from *C. reinhardtii* (21), and close to unity for that from spinach (22). Most recently, we reported an overall EET efficiency of 24% from 9-*cis*-α-carotene to Chl *a* in the Cyt *b₆f* complex from *B. corticulans* (23), which is uniquely high among the Cyt *b₆f* complexes so far studied. In this work, we have attempted to further study the EET reactions by the use of femtosecond time-resolved absorption spectroscopy.

The excited-state properties of Car are of primary importance for understanding the mechanism of Car-to-(B)Chl singlet EET. Traditionally, the $S_1(2A_g^-)$ and the $S_2(1B_u^+)$ states, respectively, are regarded as the first- and the second-lowest lying singlet excited states of Car and the $S_0(1A_g^-)$ state as the ground. The symmetric notations in parentheses are implanted from those established for conjugated linear polyene (24,25), which is the structural analog of Car. The $S_2(1B_u^+)$ state can be populated via one-photon absorption, whereas the $S_1(2A_g^-)$ state cannot because of the symmetric restriction. However, the $S_1(2A_g^-)$ state can be efficiently populated via the S_2-to-S_1 internal conversion. For photosynthetic Cars, both the $S_1(2A_g^-)$ and the $S_2(1B_u^+)$ states may conduct the Car-to-Chl EET (21,22,26) although both are extremely short lived, i.e., a few to a few tens of picoseconds for $S_1(2A_g^-)$ and ~200 fs for $S_2(1B_u^+)$. Recently, the traditional views on electronic structure and light-harvesting mechanism of Car have been challenged by the findings of a number of new intermediate excited states, e.g., the $1B_u^-$ and $3A_g^-$ state (27–30), the S* state (31,32), and the S‡ state (33). These intermediates deriving from the $S_2(1B_u^+)$ state all have unique excited-state properties and are suggested to play important roles in light harvesting. Thus the traditional picture of low-lying excited states of Car seems incomplete and is currently attracting intensive research interests (34–37).

In this work, the excited-state dynamics of all-*trans*-α-carotene free in *n*-hexane has been examined, and the α-carotene-to-Chl *a* singlet EET in the Cyt *b₆f* complex from *B. corticulans* has been shown definitively by the decay-to-rise correlation between the excited-state dynamics of α-carotene and Chl *a*. A scheme of α-carotene-to-Chl *a* singlet EET was then proposed on the basis of these results, in which $S_2(1B_u^+)$ is an efficient donor state whereas $S_1(2A_g^-)$ remains inactive. The efficient α-carotene-to-Chl *a* EET in the Cyt *b₆f* complex from *B. corticulans* may originate from the unique protein structure that is adapted to the harsh intertidal condition of light exposure. *B. corticulans* is considered a unique material for studying the possible light-assist roles of Car and Chl *a* molecules in the Cyt *b₆f* complex.

MATERIALS AND METHODS

Sample preparation

All-*trans*-α-carotene was isolated from a mixture of all-*trans*-α-carotene and all-*trans*-β-carotene (~1/2 w/w; Sigma, Steinheim, Germany) by high performance liquid chromatography (Hitachi D-7000, Hitachinaka, Japan) with an octadecyl silane C18 column (diameter 4.6 mm, length 250 mm; Alltech Associates, Deerfield, IL) and with methanol/water (9:1 v/v) as an eluent (flow rate 1 ml/min) (38). Chl *a* (~95%) and *n*-octyl-β-D-glucopyranoside (β-OG) purchased from Sigma were used as received. Rectified analytical grade *n*-hexane and acetone (Beijing Chemical Plant, Beijing, China), respectively, were used for preparing all-*trans*-α-carotene (1.6×10^{-5} M) and Chl *a* (5.3×10^{-5} M) solutions.

Wild-living marine green alga *B. corticulans* was collected from the intertidal zone at Qingdao, China. The Cyt *b₆f* complex was isolated and purified following the procedures described in detail in Li et al. (9). For time-resolved spectroscopic measurements, the *B. corticulans* Cyt *b₆f* complex was suspended in a buffer containing 50 mM tricine-NaOH and 30 mM β-OG (pH = 8.0), the optical density at the excitation wavelength of 480 nm was 0.3/mm. It has been shown that the Car molecule in the Cyt *b₆f* complex from *B. corticulans* is 9-*cis*-α-carotene and that the Chl *a*/α-carotene stoichiometric ratio in this complex is 1.2:0.9 (9,23).

Steady-state and femtosecond time-resolved absorption spectroscopies

Spectrophotometers used in steady-state spectroscopic measurements were U-3310 (Hitachi, Japan) for electronic absorption spectra and F-2500 (Hitachi) for fluorescence and fluorescence excitation spectra.

The femtosecond time-resolved absorption spectrometer has been described in detail elsewhere (39). Briefly, the output pulses (800 nm, 120 fs, 800 μJ/pulse) from a regenerative amplifier (Spitfire, Spectra Physics, Mountain View, CA) seeded with a mode-locked Ti:sapphire laser (Tsunami, Spectra Physics) were split into two components by the use of a 9:1 beam splitter. The major component was used to pump an optical parametric amplifier (OPA-800 CF, Spectra Physics) producing the excitation pulse at a desired wavelength, the pulse energy was ~200 nJ/pulse. The pump beam was focused on the sample cell with a spot size of 200 μm in diameter. The minor component was reduced to 3 μJ/pulse and focused into a 10-mm D₂O flowing cell to generate the white-light-continuum probe pulses. A band-pass filter (SPF-750, CVI) was inserted into the probe beam to select visible probe (400 ~ 700 nm) and a cutoff filter (HWB850, Nantong, China) for near-infrared probe (800 ~ 1100 nm). The magic-angle scheme was adopted in the pump-probe measurements, and the temporal resolution between the pump and the probe pulses was determined to be ~150 fs (full width at half-maximum) by the use of a nonresonant optical Kerr-effect signal. Time-resolved spectra were corrected against group velocity dispersion. The detection system was based on a liquid nitrogen cooled charge-coupled device detector (Spectrum-1, JY) attached to an imaging spectrometer (270M, SPEX). The time delay between pump and probe pulses was regulated by the use of a motorized translational stage (LTS-200, Σ-Koki) in the pump beam. To ensure that each laser shot shined on fresh sample, the laser system was run at a low repetition rate of 5 Hz, and the sample cell (optical path length, 1 mm) was kept shifting across the laser beams. All spectroscopic measurements were done at room temperature.

Time-resolved spectra were analyzed by the use of singular value decomposition (SVD) combined with model-based global fitting (SVD-Global), details of which were described elsewhere (40). The evolution-associated difference spectra (EADS) and the corresponding population dynamics, as the results of SVD-Global analysis, were used to rebuild a data matrix that was subtracted from the original data to yield a residual matrix. The quality of the SVD-Global analysis was judged by examining the residual matrix, which should be featureless and noise only, and by taking the standard deviation of least-square fitting as a criterion (41).

RESULTS AND DISCUSSION

Steady-state absorption and fluorescence spectra

All-*trans*-α-carotene (Fig. 1, *inset*) belongs to the family of C40-carotenes; its C4′=C5′ double bond in a β-ionone ring does not conjugate to the polyene backbone; and the number
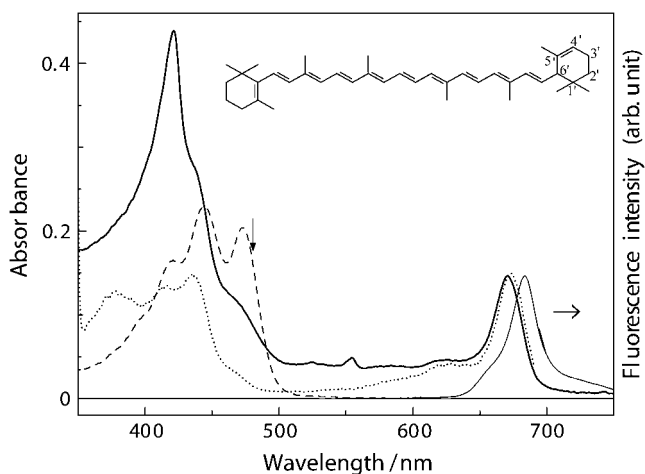
FIGURE 1 Room temperature steady-state absorption (*thicker solid line*), fluorescence (*thinner solid line*), and fluorescence excitation (*dotted line*; observing wavelength 700 nm) spectra of the Cyt b_6f complex form *B. corticulans*. The absorption spectrum of all-*trans*-α-carotene in *n*-hexane (*dashed line*) is also shown. Vertical arrow indicates the excitation wavelength (480 nm) in the time-resolved measurements. Inset shows the chemical structure of all-*trans*-α-carotene.

of conjugated C=C double bonds ($N_{C=C}$) counts 10. As seen in Fig. 1, the wavelength of $S_2(1B_u^+, v = 0) \leftarrow S_0(1A_g^-, v = 0)$ vibronic transition in the ground state absorption of all-*trans*-α-carotene in *n*-hexane is almost the same as that of 9-*cis*-α-carotene bound to the Cyt b_6f complex from *B. corticulans* ($\sim$470 nm). This contrasts to the general trend that Cars bound to pigment-protein complexes exhibit significant bathochromic shift of ground state absorption with respect to those free in *n*-hexane (31,42,43). The physical origins of the bathochromic shift in bacterial antenna complexes (20 $\sim$ 30 nm) has been suggested to be the dispersive and the electrostatic interactions with the protein environment (42,44). Therefore, the lack of spectral shift of α-carotene upon changing from *n*-hexane to the Cyt b_6f complex observed in this study suggests relatively weak interactions with its surrounding residues. As a piece of supporting evidence to the uniqueness of the protein environment in the Cyt b_6f complex from *B. corticulans*, our recent work has shown that, when this complex was denatured with sodium dodecyl sulfonate treatment, the absorption of α-carotene showed a 2-nm bathochromic shift instead of a hypsochromic shift (23).

In the absorption spectrum shown in Fig. 1, the strong absorption band at 420 nm originates from metalloporphyrin chromophores, i.e., two b-type hemes (heme b_H, heme b_L) in Cyt b_6 together with a c-type heme in Cyt f (45). The relatively weak shoulder at 436 nm corresponds to the Soret band of Chl a, and the peak at 671 nm to the well-known Q_y absorption of Chl a. In the fluorescence excitation spectrum, the 436-nm Soret band reflects efficient electronic internal conversion in Chl a, whereas the Car band at 470 nm proves

the existence of α-carotene-to-Chl a EET whose overall efficiency was estimated to be 24% (23). This efficient EET is unique to the Cyt b_6f complex from *B. corticulans* as it is not found for *C. reinhardtti* (14) or very inefficient in the Cyt b_6f complex from *M. laminosus* (7).

Singlet excited-state dynamics of all-*tran*-α-carotene free in *n*-hexane

Knowledge of the excited-state dynamics of α-carotene in the absence of an energy acceptor is crucial for studying the α-carotene-to-Chl a EET in the Cyt b_6f complex from *B. corticulans*. For this purpose, we used all-*trans*-α-carotene in *n*-hexane to mimic 9-*cis*-α-carotene in the protein environment because of the aforementioned similarity in the ground state absorptions. This is reasonable in view of the fact that a peripheral *cis*-Car has rather small reduction in effective conjugation length with respect to its all-*trans* counterpart as indicated by the small hypsochromic shift in the absorption spectrum (46,47). In addition, similar singlet excited-state kinetics may be expected for all-*trans* and peripheral *cis* isomers of a Car (48).

The time-resolved spectra in Fig. 2 for all-*trans*-α-carotene in *n*-hexane can be characterized as follows. In the visible region and immediately after the pulsed excitation (Fig. 2 *a*, 0.0 $\sim$ 0.1 ps), a sharp negative feature appears at slightly longer wavelengths ($\sim$478 nm) to the 0 $\leftarrow$ 0 transition in the ground state absorption (473 nm); this negative feature is due to the $S_2(1B_u^+) \rightarrow S_0(1A_g^-)$ stimulated emission (SE) as previously reported for lycopene and β-carotene (49,39). The SE evolves from 0.2 ps through 0.5 ps and eventually transforms into the bleach of ground state absorption (BLC). The positive feature at 0.1 ps has a rather broad spectral coverage, 500 $\sim$ 700 nm, and differs from the well-known $S_n \leftarrow S_1(2A_g^-)$ absorption seen at the picosecond delay times. This characteristic red-wing absorption was observed also for β-carotene, zeaxanthin, and lycopene (50,51), which has been attributed to the excited-state absorption (ESA) from a twisted conformer in the $S_1(2A_g^-)$ state (51) or to the ESA from higher vibrational levels in this state (50,52). In our previous study on all-*trans* neurosporene in *n*-hexane, a similar feature has been ascribed to the $1B_u^-$ state with a lifetime of $\sim$300 fs (40). The positive ESA in the near-infrared (NIR) region immediately after the pulsed excitation (Fig. 2 *b*, 0.0 $\sim$ 0.2 ps) is the characteristic ESA from the $S_2(1B_u^+)$ state (53), which shifts to the red wavelengths after 0.2 ps.

To extract the EADS spectra and the population dynamics of the excited-state intermediates giving rise to the time-resolved spectra in Fig. 2, we applied SVD-Global analyses based on a sequential kinetics model, i.e., I $\rightarrow$ II $\rightarrow$ III, in which each component stands for an independent intermediate. Fig. 3 shows the results of a three-component analysis in the visible region (*a* and *c*) and those of a two-component analysis in the NIR region (*b* and *d*).
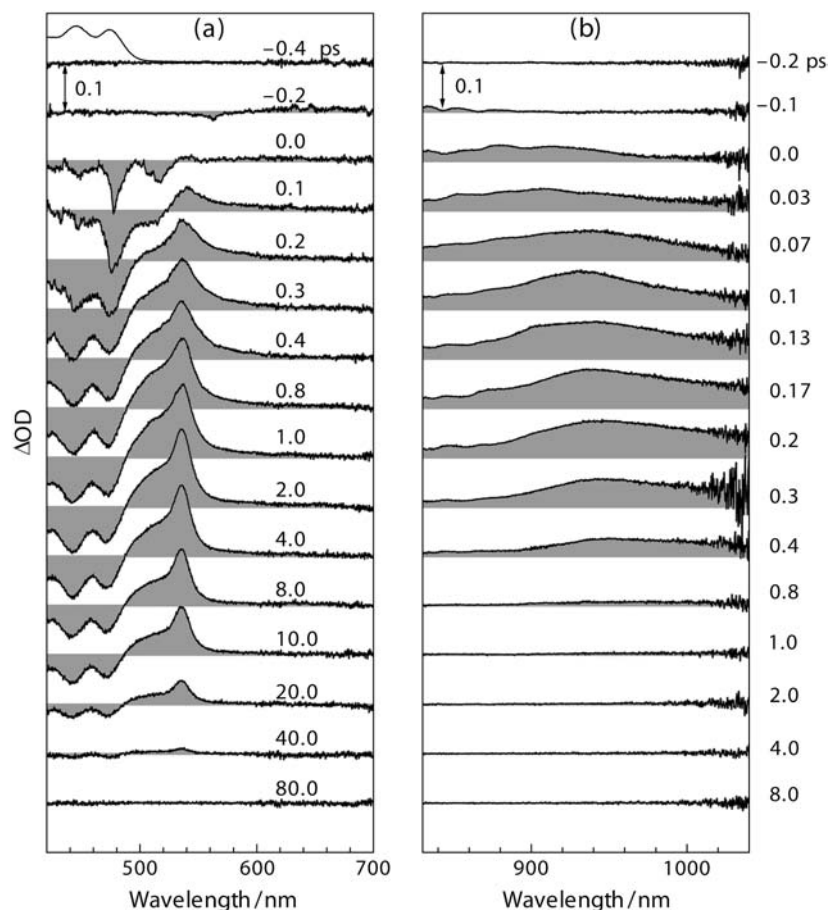
FIGURE 2 Femtosecond time-resolved absorption spectra at indicated delay times for all-*trans*-α-carotene in *n*-hexane (1.6×10^{-5} M) recorded in (*a*) the visible and (*b*) the near-infrared spectral regions.

In the visible region (Fig. 3 *a*), component-I with clear vibronic structure is ascribed to the $S_2(1B_u^+) \rightarrow S_0(1A_g^-)$ SE as supported by its mirror-image relationship with reference to the ground-state absorption (Fig. 2 *a*, *top curve*). In the NIR region, component-I exhibits a negative feature at the longer-wavelength side (>950 nm, Fig. 3 *b*). This component in the visible and the NIR regions may have the same origin because they have almost the same decay time constant of 54 ± 10 fs. Since component-I responds promptly to the pulsed excitation, it is to be attributed to the Frank-Condon active $S_2(1B_u^+)$ state of α-carotene in the initial all-*trans* configuration (vide infra).

Component-II in the visible spectral region has a decay time constant of 470 ± 40 fs which differs considerably from that of 230 ± 10 fs in the NIR region; therefore, this component in the visible and the NIR regions must have different origins. First, we consider the assignments of component-I and -II in the NIR region. In view of the lifetime of component-II (230 ± 10 fs), which is close to the reported value of $S_2(1B_u^+)$ state as determined by the use of fluorescence up-conversion techniques (~200 fs, 54,55), we ascribe this component to the $S_2(1B_u^+)$ state. The rapid transformation from component-I into -II reflects the initial configurational relaxation of the Frank-Condon active

$S_2(1B_u^+)$ state. This scheme of excited-state dynamics was originally proposed by de Weerd et al. based on time-resolved absorption spectroscopic results (51), which seems to be supported by the time-resolved fluorescence spectroscopic results obtained at ambient and cryogenic temperatures (56). Importantly, curves fitting to single-wavelength NIR kinetics revealed systematic elongation of the decay time constant at a longer wavelength, e.g., 200 ± 10 fs (850 nm), 210 ± 10 fs (900 nm), and 230 ± 10 fs (950 nm, 990 nm). Similar wavelength dependence of the decay time constant as well as the Stokes shift of ESA has also been observed for all-*trans*-β-carotene (35,53,57). These observations may be accounted for by the scheme depicted in Fig. 4, which is taken from de Weerd et al. (51) with some modifications: Along the configuration coordinate of a Car molecule, a decrease in the separation between potential energy surfaces (PES) of the $S_2(1B_u^+)$ and the S_m states explains the apparent Stokes shift of the $S_m \leftarrow S_2(1B_u^+)$ NIR absorption. In addition, the progressive elongation of the decay time constant can be explained by the rapid deviation from the initially populated Frank-Condon active state to the configurationally relaxed state along the PES of $S_2(1B_u^+)$. Within the framework of the above scheme, the negative feature in the EADS component-I (Fig. 3 *b*, >950
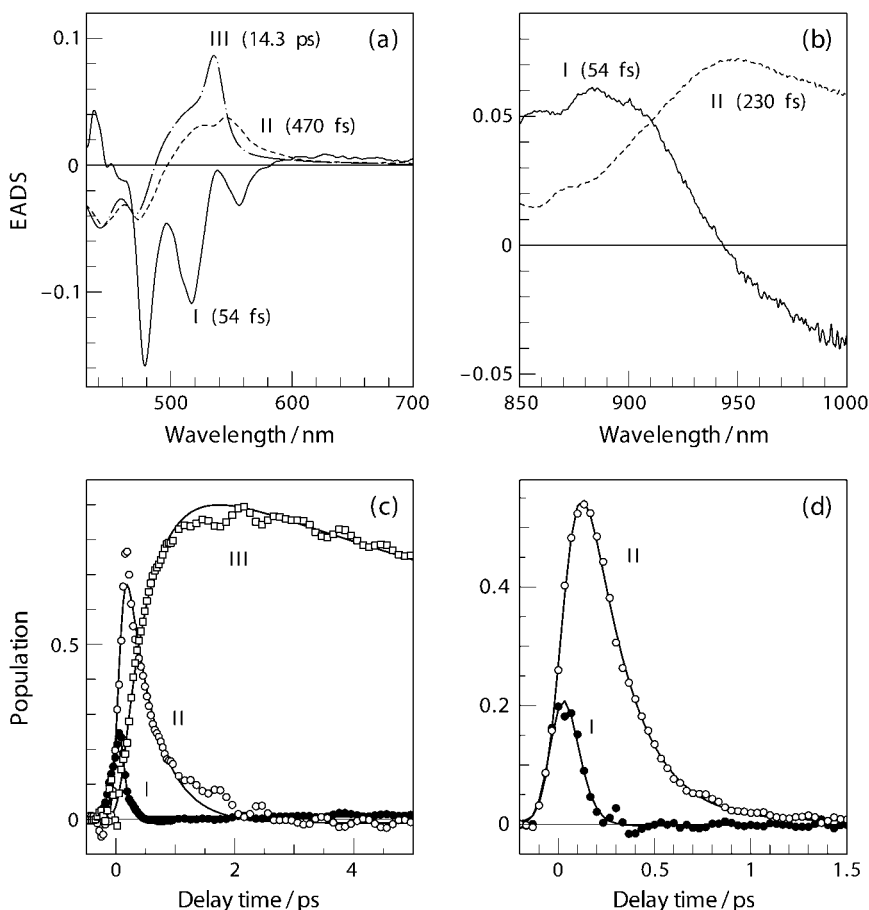
FIGURE 3 EADS and excited-state population derived from the SVD-Global analyses to the time-resolved spectra in Fig. 2 in the visible (*a* and *c*) and in the NIR (*b* and *d*) regions. Ordinal numbers indicate the order of transient species involved in the sequential kinetics model I → II → III. Lifetimes associating to the EADS components are given in parentheses.

nm) can be interpreted as a rise phase owing to the rapid relaxation of the initially populated Frank-Condon active $S_2(1B_u^+)$ state.

In an alternative explanation to the aforementioned ultra-fast spectral changes, the $1B_u^-$ state located between the $S_2(1B_u^+)$ and the $S_1(2A_g^-)$ states and derived directly from the $S_2(1B_u^+)$ state was taken into account and was suggested to mediate the S_2-to-S_1 internal conversion. According to this scheme, the lifetimes of the $1B_u^-$ and the $1B_u^+$ states were proposed to be on the timescales of ~10 fs and ~200 fs (58,57), respectively. It is argued, however, that the ultrafast spectral changes can also be simply explained in terms of rapid moving out of the Frank-Condon active region owing to the initial nuclear relaxation (possibly mediated by certain vibrational modes). In addition, given the small energy separation (state mixing is therefore significant) between the $1B_u^-$ and the $1B_u^+$ states, they can hardly be distinguished by the use of femtosecond excitation pulse with rather broad-band width (35). Obviously, further investigation in terms of not only dynamics but also energetics is necessary to clarify the nature of the intermediate states. Here, we note that either the spectral dynamics mentioned above or those to be described below can be well accounted for by invoking the scheme depicted in Fig. 4.

We now consider component-II in the visible region with a lifetime of 470 ± 40 fs. This EADS component can be attributed to the configurationally unrelaxed $S_1(2A_g^-)$ state that directly converted from the configurationally distorted $S_2(1B_u^+)$ state (Fig. 4). Its lifetime is also close to the reported timescale of the vibronical relaxation in $S_1(2A_g^-)$ state (50). Either the configurationally or the vibrationally unrelaxed $S_1(2A_g^-)$ state may be referred to as the hot S_1 in a sense that it carries excess excitation energy. Finally, component-III in Fig. 3 *a* with a lifetime of 14.3 ± 0.4 ps is definitively assigned to the $S_1(2A_g^-)$ state; this EADS component faithfully reflects the characteristic ESA of $S_n ← S_1(2A_g^-)$ as seen at later delay times in Fig. 2 *a*. Its lifetime determined by the use of SVD-Global analysis agrees well with that obtained from a single kinetics curve at 535 nm (14.7 ± 0.9 ps, see Fig. 6 *a*).

Singlet EET from α-carotene to Chl *a* in the *B. corticulans* Cyt b_6f complex

To investigate the detailed paths and mechanisms of the EET reactions, we selectively excited α-carotene in the Cyt b_6f complex by using femtosecond pulse at 480 nm, i.e., the longer wavelength side of the 0 ← 0 vibronic band of
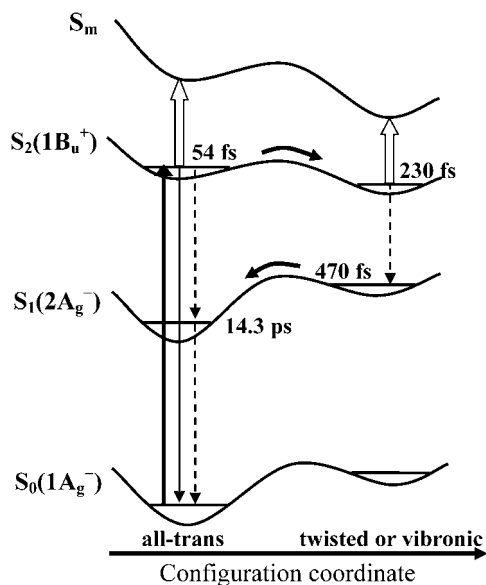
FIGURE 4 Schematic illustration of the excited-state dynamics of all-*trans*-α-carotene from de Weerd et al. (51) with some modifications. The indicated decay time constants of the relevant transient species were derived from the SVD-Global analyses (see text for details). Thicker solid arrow stands for optical excitation and configurational relaxation, thinner solid arrow for the $S_2(1B_u^+) \rightarrow S_0(1A_g^-)$ emissive transition, dashed arrows for internal conversion, and open arrows for the NIR transitions $S_m \leftarrow S_2(1B_u^+)$. In this scheme, the initially populated $S_2(1B_u^+)$ state in all-*trans* configuration (54 fs) relaxes rapidly into its twisted form (230 fs) and then internally converts to the twisted $S_1(2A_g^-)$ (470 fs), which eventually relaxes into the relaxed $S_1(2A_g^-)$ state (14.3 ps).
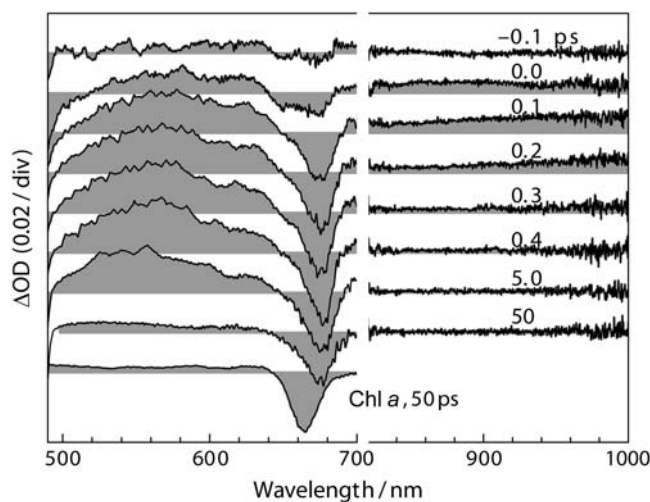

FIGURE 5 Femtosecond time-resolved absorption spectra at representative delay times recorded for the Cyt b_6f complex from *B. corticulans* ($OD_{480nm} = 0.3$/mm). For comparison, the transient spectrum for free Chl a in acetone (5.3×10^{-5} M) recorded at 50 ps under the excitation wavelength of 670 nm is shown at the bottom.

α-carotene absorption (Fig. 1, *vertical arrow*). The time-resolved absorption spectra for the Cyt b_6f complex at representative delay times are shown in Fig. 5.

Immediately after the pulsed excitation ($-0.1 \sim 0.1$ ps), broad ESAs appear at both visible wavelengths ($500 \sim 640$ nm) and NIR wavelengths ($800 \sim 1000$ nm). The visible ESA rising up until 0.4 ps and decaying out until 50 ps was mainly contributed by the $S_n \leftarrow S_1(2A_g^-)$ absorption, whereas the extremely short-lived NIR signal disappearing completely at 0.4 ps originated from the $S_2(1B_u^+)$ state. In the visible region, the transient spectrum of the Cyt b_6f complex at 50 ps is similar to that of Chl a free in organic solvent, indicating that the much stronger visible ESA at earlier delay times mainly originate from the singlet excited state of α-carotene. Most importantly, the negative BLC signal of Chl a at 675 nm responds instantaneously to the pulsed excitation (see the spectrum at 0.0 ps), a fact that strongly suggests the presence of ultrafast α-carotene-to-Chl a EET. To confirm that the amount of direct excitation of Chl a is negligible, we used the same excitation energy to selectively excite β-carotene in the Cyt b_6f complex from spinach where β-carotene-to-Chl a EET is known to be absent; no BLC signal of Chl a could be recognized.

To examine whether or not the $S_1(2A_g^-)$ state is involved in the α-carotene-to-Chl a EET, we compared the kinetics

at 570 nm for the Cyt b_6f complex from *B. corticulans* with that at 535 nm for free α-carotene (Fig. 6 a). Biexponential fitting to the kinetics of the Cyt b_6f complex found a short-lived component (14.7 ± 0.9 ps) and a nanosecond one, which can be definitively assigned to the $S_1(2A_g^-)$ state of α-carotene and to the Q_y state of Chl a, respectively. Since the lifetime of $S_1(2A_g^-)$ state shows no reduction upon changing from *n*-hexane solution (14.3 ± 0.4 ps) to the Cyt b_6f complex (14.7 ± 0.9 ps), it is concluded that this state is inactive in transferring electronic excitation to Chl a. This is understandable in view of the tiny oscillator strength of the optically forbidden $S_1(2A_g^-)$ state (59) and the large Car-Chl spatial separation of 14 Å (4,5).

The Car(S_1)-to-Chl single EET pathway has been previously reported for the LHC II (60) and the CP29 (61) complexes, in which either vibrationally unrelaxed or relaxed $S_1(2A_g^-)$ states are involved in the EET reactions. However, these processes account only for a minor part of the overall EET efficiency; the overwhelming part of energy transfer proceeds from the $S_2(1B_u^+)$ state. In this study, the involvement of the hot S_1 in the Car-to-Chl EET process seems less possible for the aforementioned structural reason as well as the following kinetics reason. In Fig. 6 a, a rise time constant of 690 ± 70 fs is found for free α-carotene, which is understandable from the scheme in Fig. 4 showing two tandem processes with the time constants of 230 fs and 470 fs, respectively. On the other hand, a rise time constant of 360 ± 50 fs is found for the Cyt b_6f complex. Although the rise time is considerably shortened in the Cyt b_6f complex, we cannot say with certainty that this is due to the energy transfer from the hot S_1 state, because the Car(S_2)-to-Chl EET process would also significantly shorten the rise time in the Cyt b_6f complex.

To determine the rate constant of singlet EET from the $S_2(1B_u^+)$ state of α-carotene to Chl a, we probe the ESA of α-carotene at 950 nm, where Chl a has little contribution, and probe the BLC of Chl a at 675 nm as shown in Fig. 6 b. Both of the kinetics were plotted directly from the time-resolved spectra in Fig. 5. Because 950 nm is around the isosbestic point of component-I (Fig. 3 b), the kinetics at this wavelength is least affected by the Stokes shift in the ESA compared to those at other wavelengths. It is clear in Fig. 6 b that the decay of the ESA of α-carotene correlates well to the rise of the BLC of Chl a; however, the rise phase in the 675-nm kinetics is obviously slower than the decay of the 950-nm one, which may be due to the Q_x-to-Q_y internal conversion process in the Chl a molecule. As shown in Fig. 6 c, the existence of singlet EET from the $S_2(1B_u^+)$ state of α-carotene to Chl a is also manifested by directly comparing the 950-nm kinetics of α-carotene in n-hexane with that in the Cyt b_6f complex. The significant reduction in the apparent decay time constants, i.e., from 230 ± 70 fs to 110 ± 30 fs (results from a single wavelength curve fitting), suggests the presence of Car(S_2)-to-Chl a EET.

The Car(S_2)-to-Chl $a(Q_x)$ pathway proposed in Fig. 6 b is consistent with the detailed kinetics schemes of the Car-to-Chl energy transfer previously proposed for the Chl-a/b light-harvesting complexes, e.g., the LHC II complex (60), the CP29 complex (61), and the Lhca4 complex from PS I (62). For all of these complexes, the $S_2(1B_u^+)$ state is responsible for a major part of the overall Car-to-Chl EET. Croce et al. (60) proposed for the first time, to our knowledge, that the Q_x is the acceptor state of Chl a, whereas both B_x and Q_x are the acceptors of Chl b.

The traces in Fig. 6 b were simultaneously fit to a kinetics model shown as an inset. In the case where the three rate constants were left as free-fitting parameters, we obtained $K_{IC} = (220 \pm 50 \text{ fs})^{-1}$, $K_{EET} = (250 \pm 90 \text{ fs})^{-1}$, and $K_{xy} = (120 \pm 10 \text{ fs})^{-1}$. Here, the time constant of S_2-to-S_1 internal conversion, 220 ± 50 fs, is very close to that found for α-carotene in n-hexane (230 ± 10 fs). Alternatively, if we fix K_{IC} at $(230 \pm 10 \text{ fs})^{-1}$, the values of K_{EET} and K_{xy} were found to be $(240 \pm 40 \text{ fs})^{-1}$ and $(130 \pm 20 \text{ fs})^{-1}$, respectively. The above two sets of rate constants are rather similar. We use the later set to evaluate the partial efficiency (η) of singlet EET from the $S_2(1B_u^+)$ state of α-carotene to the Q_x state of Chl a, and a value of $(49 \pm 4)\%$ was obtained by using the relation $\eta = K_{EET}/(K_{EET} + K_{IC})$. The rather high partial efficiency strongly supports the overall α-carotene-to-Chl a EET efficiency of 24% in the Cyt b_6f complex from $B.$ $corticulans$. As shown in Fig. 4, the S_2-to-S_1 internal conversion may occur before the relaxation of the $S_2(1B_u^+)$ state, a deactivation process which effectively competes with the EET from the relaxed $S_2(1B_u^+)$ state to the Q_x state. This explains the apparent discrepancy between the partial and the overall efficiency, i.e., 49% vs. 24%. By using the values of EET efficiency, it is estimated that $\sim$50% of the Frank-Condon active $S_2(1B_u^+)$ state goes to the
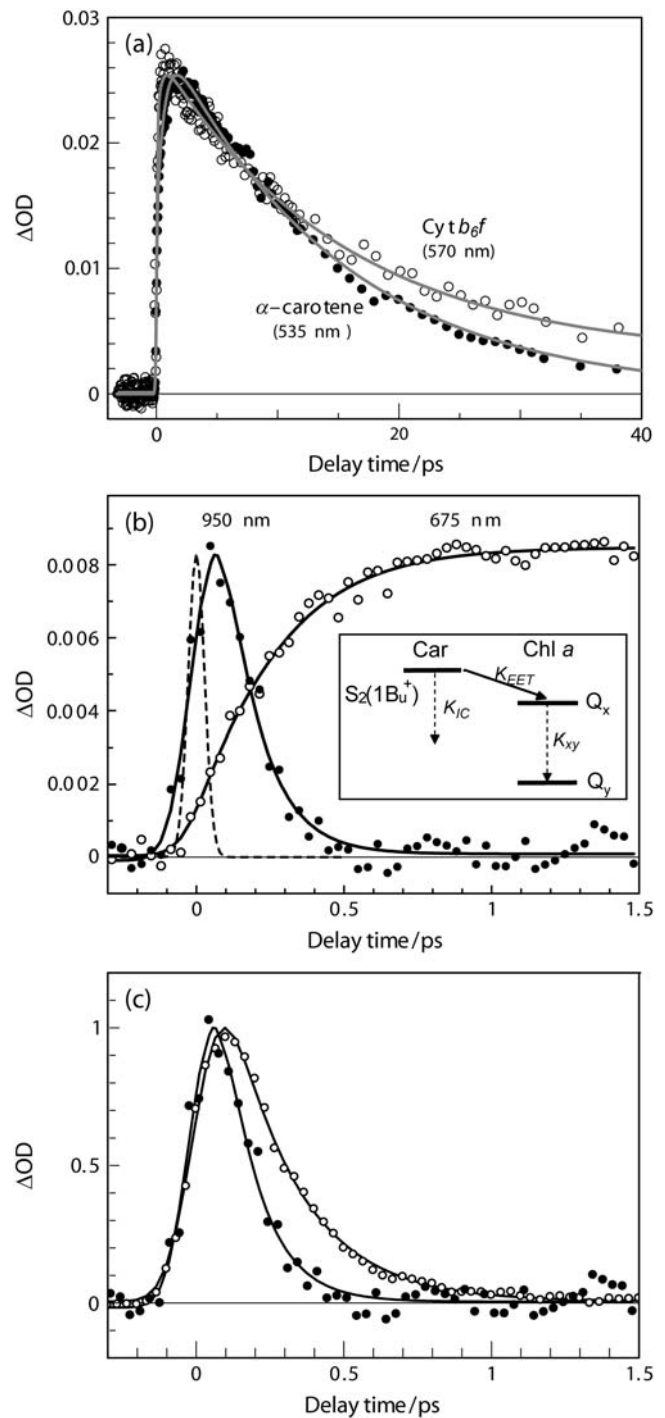

FIGURE 6 (a) Comparison of the kinetics trace at 570 nm for the Cyt b_6f complex from $B.$ $corticulans$ with that at 535 nm for α-carotene in n-hexane. (b) Kinetics traces at 675 nm (inverted and normalized by multiplying by a factor of -0.4) and at 950 nm plotted from the original time-resolved spectra (Fig. 5). They were simultaneously fit to a kinetic model depicted in the inset (K_{IC} and K_{xy} stand for the rate of internal conversion of α-carotene and Chl a, respectively, K_{EET} for the rate of energy transfer). In this scheme, the $S_2(1B_u^+)$ state is configurationally relaxed. The solid line presents fitting curve; the dashed line shows a Gaussian-type instrumental response function. (c) Comparison of the kinetics traces at 950 nm for α-carotene in n-hexane (open circle) and for the Cyt b_6f complex from $B.$ $corticulans$ (solid circle).

configurationally relaxed form, which subsequently transfers singlet excitation energy to the Q_x state of Chl a.

SUMMARY

We have examined the singlet excited-state dynamics of α-carotene both free in solution and bound in the Cyt b_6f complex from *B. corticulans* by using femtosecond time-resolved absorption spectroscopy. For free all-*trans*-α-carotene, the lifetimes of the $S_1(2A_g^-)$ and the $S_2(1B_u^+)$ states are determined to be 14.3 ± 0.4 ps and 230 ± 10 fs, respectively. These two excited states both experienced rapid configurational relaxation (Fig. 4), and their configurational precursors live on 470 ± 40 fs and 54 ± 10 fs, respectively. For the Cyt b_6f complex from *B. corticulans*, definitive spectroscopic evidence shows that the $S_2(1B_u^+)$ state of 9-*cis*-α-carotene transfers singlet excitations to the Q_x state of Chl a, whereas the $S_1(2A_g^-)$ state remains inactive. The timescale and the efficiency of EET from the $S_2(1B_u^+)$ are estimated to be $\sim$240 fs and $\sim$49%, respectively. The inset in Fig. 6 b illustrates the proposed scheme of α-carotene-to-Chl a singlet EET.

The physiological functions of Car and Chl a molecules in the Cyt b_6f complex have been attracting considerable research interests. A number of recent findings point to the photoprotective role of Car although detailed mechanisms remain unsolved. For instance, β-carotene was found to be able to protect Chl a against photobleach in the spinach Cyt b_6f complex (7) and to quench the triplet Chl a sensitized singlet oxygen in the Cyt b_6f complex from *M. laminosus*, which is likely facilitated by an oxygen diffusion channel (63). In addition, it is reported that Chl a singlet excitation was quenched by its neighboring amino acids in the Cyt b_6f complex from *Synechosystis* sp. PCC 6803, a process leading to a pronounced decrease in the yield of triplet Chl a (13). Most recently, the structural roles have been suggested for either of the pigments (64).

This work confirms the light-harvesting function of α-carotene in the Cyt b_6f complex from *B. corticulans*. As mentioned in the introduction, the Car-to-Chl singlet EET in the Cyt b_6f complex seems to be species dependent, which is likely due to the structural difference in the pigment-protein assemblies of Cyt b_6f complexes from different species. For the marine green alga *B. corticulans* living in the intertidal zone, a unique mechanism of Car-to-Chl singlet EET may be developed in its Cyt b_6f complex in response to the harsh light-exposure condition. In general, the light-harvesting function of Car is of particular importance for aquatic photosynthetic organisms, because Cars intensely absorb light at blue-green wavelengths coinciding with the spectral window of water. It is interesting to study the fate of the light excitation harvested by the Cyt b_6f complex of *B. corticulans*.

REFERENCES

1. Cramer, W. A., M. T. Black, W. R. Widger, and M. E. Girvin. 1987. Structure and function of photosynthetic cytochrome bc_1 and b_6f complexes. *In* The Light Reaction. J. Barber, editor. Elsevier, Amsterdam. 447–493.

2. Hope, A. B. 1993. The chloroplast cytochrome *bf* complex: a critical focus on function. *Biochim. Biophys. Acta.* 1143:1–22.

3. Anderson, J. M. 1992. Cytochrome b_6f complex: dynamic molecular organization, function and acclimation. *Photosynth. Res.* 34:341–357.

4. Kurisu, G., H. Zhang, J. L. Smith, and W. A. Cramer. 2003. Structure of the cytochrome b_6f complex of oxygenic photosynthesis: tuning the cavity. *Science.* 302:1009–1014.

5. Stroebel, D., Y. Choquet, J. L. Popot, and D. Picot. 2003. An atypical haem in the cytochrome b_6f complex. *Nature.* 426:413–418.

6. Yan, J., Y. Liu, D. Mao, L. Li, and T. Kuang. 2001. The presence of 9-*cis*-β-carotene in cytochrome b_6f complex from spinach. *Biochim. Biophys. Acta.* 1506:182–188.

7. Zhang, H., D. Huang, and W. A. Cramer. 1999. Stoichiometrically bound β-carotene in the cytochrome b_6f complex of oxygenic photosynthesis protects against oxygen damage. *J. Biol. Chem.* 274: 1581–1587.

8. Boronowsky, U., S. O. Wenk, D. Schneider, C. Jäger, and M. Rögner. 2001. Isolation of membrane protein subunits in their native state: evidence for selective binding of chlorophyll and carotenoid to the b_6 subunit of the cytochrome b_6f complex. *Biochim. Biophys. Acta.* 1506: 55–66.

9. Li, B., D. Mao, Y. Liu, L. Li, and T. Kuang. 2005. Characterization of the cytochrome b_6f complex from marine green algae, *Bryopsis corticulans. Photosynth. Res.* 83:297–305.

10. Frank, H. A., and R. J. Cogdell. 1993. Photochemistry and functions of carotenoids in photosynthesis. *In* Carotenoids in Photosynthesis. A. Young and G. Britton editors. Springer Verlag, London. 252–326.

11. Ritz, T., A. Damjanović, K. Schulten, J. P. Zhang, and Y. Koyama. 2000. Efficient light harvesting through carotenoids. *Photosynth. Res.* 66:125–144.

12. Soriano, G. M., M. V. Ponamarev, C. J. Carrell, D. Xia, J. L. Smith, and W. A. Cramer. 1999. Comparison of the cytochrome bc_1 complex with the anticipated structure of the cytochrome b_6f complex: de plus ça change de plus c'est la même chose. *J. Bioenerg. Biomembr.* 31:201–213.

13. Peterman, E. J. G., S. O. Wenk, T. Pullerits, L. O. Pålsson, R. van Grondelle, J. P. Dekker, M. Rögner, and H. van Amerongen. 1998. Fluorescence and absorption spectroscopy of the weakly fluorescent Chlorophyll a in Cytochrome b_6f of *Synechocystis PCC6803. Biophys. J.* 75:389–398.

14. Pierre, Y., C. Breyton, Y. Lemoine, B. Robert, C. Vernotte, and J. L. Popot. 1997. On the presence and role of a molecule of chlorophyll a in the cytochrome b_6f complex. *J. Biol. Chem.* 272:21901–21908.

15. Cramer, W. A., H. Zhang, J. Yan, G. Kurisu, and J. L. Smith. 2004. Evolution of photosynthesis: time-independent structure of the cytochrome b_6f complex. *Biochemistry.* 43:5921–5929.

16. Cramer, W. A., J. Yan, H. Zhang, G. Kurisu, and J. L. Smith. 2005. Structure of the cytochrome b_6f complex: new prosthetic groups, Q-space, and the 'hors d'oeuvres hypothesis' for assembly of the complex. *Photosynth. Res.* 85:133–144.

17. Polívka, T., and V. Sundström. 2004. Ultrafast dynamics of carotenoid excited states—from solution to natural and artificial systems. *Chem. Rev.* 104:2021–2071.

18. Lin, S., E. Katilius, A. K. W. Taguchi, and N. W. Woodbury. 2003. Excitation energy transfer from carotenoid to bacteriochlorophyll in the

photosynthetic purple bacterial reaction center of *Rhodobacter sphaeroides*. *J. Phys. Chem. B.* 107:14103–14108.

19. Holt, N. E., J. T. M. Kennis, and G. R. Fleming. 2004. Femtosecond fluorescence upconversion studies of light harvesting by β-carotene in oxygenic photosynthetic core proteins. *J. Phys. Chem. B.* 108:19029–19035.

20. de Weerd, F. L., J. P. Dekker, and R. van Grondelle. 2003. Dynamics of β-carotene-to-chlorophyll singlet energy transfer in the core of photosystem II. *J. Phys. Chem. B.* 107:6214–6220.

21. Walla, P. J., J. Yom, B. P. Krueger, and G. R. Fleming. 2000. Two-photon excitation spectrum of light-harvesting complex II and fluorescence upconversion after one- and two-photon excitation of the carotenoids. *J. Phys. Chem. B.* 104:4799–4806.

22. Gradinaru, C. C., I. H. M. van Stokkum, A. A. Pascal, R. van Grondelle, and H. van Amerongen. 2000. Identifying the pathways of energy transfer between carotenoids and chlorophylls in LHCII and CP29. A multicolor, femtosecond pump-probe study. *J. Phys. Chem. B.* 104:9330–9342.

23. Li, B. X., P. Zuo, X. B. Chen, L. B. Li, J. P. Zhang, and T. Y. Kuang. 2005. Study on energy transfer between carotenoid and chlorophyll *a* in cytochrome b_6f complex from *Bryopsis corticulans*. *Photosynth. Res.* In press.

24. Hudson, B. S., B. E. Kohler, and K. Schulten. 1982. Linear polyene electronic structure and potential surfaces. *In* Excited States. E. C. Lim, editor. Academic Press, New York. 1–95.

25. Tavan, P., and K. Schulten. 1987. Electronic excitations in finite and infinite polyenes. *Phys. Rev. B.* 36:4337–4358.

26. Walla, P. J., P. A. Linden, C. P. Hsu, G. D. Scholes, and G. R. Fleming. 2000. Femtosecond dynamics of the forbidden carotenoid S_1 state in light-harvesting complexes of purple bacteria observed after two-photon excitation. *Proc. Natl. Acad. Sci. USA.* 97:10808–10813.

27. Sashima, T., H. Nagae, M. Kuki, and Y. Koyama. 1999. A new singlet-excited state of all-*trans*-spheroidene as detected by resonance-Raman excitation profiles. *Chem. Phys. Lett.* 299:187–194.

28. Fujii, R., T. Inaba, Y. Watanabe, Y. Koyama, and J. P. Zhang. 2003. Two deferent pathways of internal conversion in carotenoids depending on the length of the conjugated chain. *Chem. Phys. Lett.* 369:165–172.

29. Rondonuwu, F. S., Y. Watanabe, R. Fujii, and Y. Koyama. 2003. A first detection of singlet to triplet conversion from the $1^1B_u^-$ to the 1^3A_g state and triplet internal conversion from the 1^3A_g to the 1^3B_u state in carotenoids: dependence on the conjugation length. *Chem. Phys. Lett.* 376:292–301.

30. Polli, D., G. Cerullo, G. Lanzani, S. De Silvestri, K. Yanagi, H. Hashimoto, and R. J. Cogdell. 2004. Conjugation length dependence of internal conversion in carotenoids: role of the intermediate state. *Phys. Rev. Lett.* 93:163002.

31. Gradinaru, C. C., J. T. M. Kennis, E. Papagiannakis, I. H. M. van Stokkum, R. J. Cogdell, G. R. Fleming, R. A. Niederman, and R. van Grondelle. 2001. An unusual pathway of excitation energy deactivation in carotenoids: singlet-to-triplet conversion on an ultrafast timescale in a photosynthetic antenna. *Proc. Natl. Acad. Sci. USA.* 98:2364–2369.

32. Papagiannakis, E., J. T. M. Kennis, I. H. M. van Stokkum, R. J. Cogdell, and R. van Grondelle. 2002. An alternative carotenoid-to-bacteriochlorophyll energy transfer pathway in photosynthetic light harvesting. *Proc. Natl. Acad. Sci. USA.* 99:6017–6022.

33. Larsen, D. S., E. Papagiannakis, I. H. M. van Stokkum, M. Vengris, J. T. M. Kennis, and R. van Grondelle. 2003. Excited state dynamics of β-carotene explored with dispersed multi-pulse transient absorption. *Chem. Phys. Lett.* 381:733–742.

34. Kodis, G., C. Herrero, R. Palacios, E. Marino-Ochoa, S. Gould, L. de la Garza, R. van Grondelle, D. Gust, T. A. Moore, A. L. Moore, and J. T. M. Kennis. 2004. Light harvesting and photoprotective functions of carotenoids in compact artificial photosynthetic antenna designs. *J. Phys. Chem. B.* 108:414–425.

35. Kukura, P., D. W. McCamant, and R. A. Mathies. 2004. Femtosecond time-resolved stimulated Raman spectroscopy of the S_2 ($1B_u^+$) excited state of β-carotene. *J. Phys. Chem. A.* 108:5921–5925.

36. Hashimoto, H., K. Yanagi, M. Yoshizawa, D. Polli, G. Cerullo, G. Lanzani, S. de Silvestri, A. T. Gardiner, and R. J. Cogdell. 2004. The very early events following photoexcitation of carotenoids. *Arch. Biochem. Biophys.* 430:61–69.

37. Papagiannakis, E., M. Vengris, D. S. Larsen, I. H. M. van Stokkum, R. G. Hiller, and R. van Grondelle. 2006. Use of ultrafast dispersed pump-dump-probe and pump-repump-probe spectroscopies to explore the light-induced dynamics of peridinin in solution. *J. Phys. Chem. B.* 110:512–521.

38. Ortega, H., J. L. Coperias, P. Castilla, D. Gómez-Coronado, and M. A. Lasunción. 2004. Liquid chromatographic method for the simultaneous determination of different lipid-soluble antioxidants in human plasma and low-density lipoproteins. *J. Chromatogr. B Analyt. Technol. Biomed. Life Sci.* 803:249–255.

39. Han, R. M., Y. S. Wu, J. Feng, X. C. Ai, J. P. Zhang, and L. H. Skibsted. 2004. Radical cation generation from singlet and triplet excited states of all-*trans*-lycopene in chloroform. *Photochem. Photobiol.* 80:326–333.

40. Zhang, J. P., T. Inaba, Y. Watanabe, and Y. Koyama. 2000. Sub-picosecond time-resolved absorption spectroscopy of all-*trans*-neurosporene in solution and bound to the LH2 complex from *Rhodobacter sphaeroides* G1C. *Chem. Phys. Lett.* 331:154–162.

41. Zhang, J. P., T. Inaba, Y. Watanabe, and Y. Koyama. 2000. Excited-state dynamics among the $1B_u^+$, $1B_u^-$ and $2A_g^-$ states of all-*trans*-neurosporene as revealed by near-infrared time-resolved absorption spectroscopy. *Chem. Phys. Lett.* 332:351–358.

42. Andersson, P. O., T. Gillbro, L. Ferguson, and R. J. Cogdell. 1991. Absorption spectral shifts of carotenoids related to medium polarizability. *Photochem. Photobiol.* 54:353–360.

43. Cianci, M., P. J. Rizkallah, A. Olczak, J. Raftery, N. E. Chayen, P. F. Zagalsky, and J. R. Helliwell. 2002. The molecular basis of the coloration mechanism in lobster shell: beta-crustacyanin at 3.2-Å resolution. *Proc. Natl. Acad. Sci. USA.* 99:9795–9800.

44. Wang, Y., and X. Hu. 2002. A quantum chemistry study of binding carotenoids in the bacterial light-harvesting complexes. *J. Am. Chem. Soc.* 124:8445–8451.

45. Picaud, T., C. L. Moigne, A. G. de Gracia, and A. Desbois. 2001. Soret-excited Raman spectroscopy of the spinach cytochrome b_6f complex. Structures of the *b*- and *c*-type hemes, chlorophyll *a*, and β-carotene. *Biochemistry.* 40:7309–7317.

46. Fujii, R., C. H. Chen, T. Mizoguchi, and Y. Koyama. 1998. ^{1}HNMR, electronic-absorption and resonance-Raman spectra of isomeric okenone as compared with those of isomeric β-carotene, canthaxanthin, β-apo-8′-carotenal and spheroidene. *Spectrochim. Acta A Mol. Biomol. Spectrosc.* 54:727–743.

47. Fujii, R., T. Ishikawa, Y. Koyama, M. Taguchi, Y. Isobe, H. Nagae, and Y. Watanabe. 2001. Fluorescence spectroscopy of all-*trans*-anhydrorhodovibrin and spirilloxanthin: detection of the $1B_u^-$ fluorescence. *J. Phys. Chem. A.* 105:5348–5355.

48. Hashimoto, H., Y. Koyama, Y. Hirata, and N. Mataga. 1991. S_1 and T_1 species of β-carotene generated by direct photoexcitation from the all-*trans*, 9-*cis*, 13-*cis*, and 15-*cis* isomers as revealed by picosecond transient absorption and transient Raman spectroscopies. *J. Phys. Chem.* 95:3072–3076.

49. Zhang, J. P., R. Fujii, Y. Koyama, F. S. Rondonuwu, Y. Watanabe, A. Mortensen, and L. H. Skibsted. 2001. The $1B_u$-type singlet state of β-carotene as a precursor of the radical cation found in chloroform solution by sub-picosecond time-resolved absorption spectroscopy. *Chem. Phys. Lett.* 348:235–241.

50. Billsten, H. H., D. Zigmantas, V. Sundström, and T. Polívka. 2002. Dynamics of vibrational relaxation in the S_1 state of carotenoids having 11 conjugated C=C bonds. *Chem. Phys. Lett.* 355:465–470.

51. de Weerd, F. L., I. H. M. van Stokkum, and R. van Grondelle. 2002. Subpicosecond dynamics in the excited state absorption of all-*trans*-β-carotene. *Chem. Phys. Lett.* 354:38–43.

52. Yoshizawa, M., H. Aoki, and H. Hashimoto. 2001. Vibrational relaxation of the $2A_g^-$ excited state in all-*trans*-beta-carotene obtained

by femtosecond time-resolved Raman spectroscopy. *Phys. Rev. B.* 63:180301–180304.

53. Zhang, J. P., L. H. Skibsted, R. Fujii, and Y. Koyama. 2001. Transient absorption from the $1B_u^+$ state of all-*trans*-β-carotene newly identified in the near-infrared region. *Photochem. Photobiol.* 73:219–222.

54. Kandori, H., H. Sasabe, and M. Mimuro. 1994. Direct determination of a lifetime of the S_2 state of β-carotene by femtosecond time-resolved fluorescence spectroscopy. *J. Am. Chem. Soc.* 116:2671–2672.

55. Akimoto, S., I. Yamazaki, S. Takaichi, and M. Mimuro. 1999. Excitation relaxation of carotenoids within the S_2 state probed by the femtosecond fluorescence up-conversion method. *Chem. Phys. Lett.* 313:63–68.

56. Akimoto, S., I. Yamazaki, T. Sakawa, and M. Mimuro. 2002. Temperature effects on excitation relaxation dynamics of the carotenoid β-carotene and its analogue β-Apo-8′-carotenal, probed by femtosecond fluorescence spectroscopy. *J. Phys. Chem. A.* 106:2237–2243.

57. Cerullo, G., D. Polli, G. Lanzani, S. De Silvetri, H. Hashimoto, and R. J. Cogdell. 2002. Photosynthetic light harvesting by carotenoids: detection of an intermediate excited states. *Science.* 298:2395–2398.

58. Koyama, Y., F. S. Rondonuwu, R. Fujii, and Y. Watanabe. 2004. Light-harvesting function of carotenoids in photo-synthesis: the roles of the newly found $1^1B_u^-$ state. *Biopolymers.* 74:2–18.

59. Zhang, J. P., R. Fujii, P. Qian, T. Inaba, T. Mizoguchi, Y. Koyama, K. Onaka, Y. Watanabe, and H. Nagae. 2000. Mechanism of the carotenoid-to-bacteriochlorophyll energy transfer via the S_1 state in the LH2 complexes from purple bacteria. *J. Phys. Chem. B.* 104:3683–3691.

60. Croce, R., M. G. Müller, R. Bassi, and A. R. Holzwarth. 2001. Carotenoid-to-chlorophyll energy transfer in recombinant major light-harvesting complex (LHCII) of higher plants. I. Femtosecond transient absorption measurements. *Biophys. J.* 80:901–915.

61. Croce, R., M. G. Müller, S. Caffarri, R. Bassi, and A. R. Holzwarth. 2003. Energy transfer pathways in the minor antenna complex CP29 of photosystem II: a femtosecond study of carotenoid to chlorophyll transfer on mutant and WT complexes. *Biophys. J.* 84:2517–2532.

62. Gibasiewicz, K., R. Croce, T. Morosinotto, J. A. Ihalainen, I. H. M. van Stokkum, J. P. Dekker, R. Bassi, and R. van Grondelle. 2005. Excitation energy transfer pathways in Lhca4. *Biophys. J.* 88:1959–1969.

63. Kim, H., N. Dashdorj, H. Zhang, J. Yan, W. A. Cramer, and S. Savikhin. 2005. An anomalous distance dependence of intra-protein chlorophyll-carotenoid triplet energy transfer. *Biophys. J.* 89:L28–L30.

64. Wenk, S. O., D. Schneider, U. Boronowsky, C. Jäger, C. Klughammer, F. L. de Weerd, H. van Roon, W. F. J. Vermaas, J. P. Dekker, and M. Rögner. 2005. Functional implications of pigments bound to a cyanobacterial cytochrome b_6f complex. *FEBS J.* 272:582–592.